

## FIRST LASING OF THE ELBE MID-IR FEL

P. Michel, F. Gabriel, E. Grosse, P. Evtushenko, T. Dekorsy, M. Krenz, M. Helm,  
U. Lehnert, W. Seidel, R. Wünsch, D. Wohlfarth, A. Wolf  
Forschungszentrum Rossendorf, Germany

### Abstract

First lasing of the mid-infrared free-electron laser at ELBE was achieved on May 7, 2004. The Radiation Source ELBE at the Forschungszentrum Rossendorf in Dresden is currently under transition from commissioning to regular user operation. Presently the electron linac produces an up to 18 MeV, 1 mA (cw) electron beam which is allotted to generate various kinds of secondary radiation. After the successful commissioning of the bremsstrahlung and channeling-X-ray facilities during 2003 stable lasing has now been observed in the IR range (15 to 22  $\mu\text{m}$ ). The oscillator FEL is equipped with two planar undulator units, both consisting of 34 hybrid permanent magnets with a period of 27.3 mm ( $K_{rms} = 0.3 \dots 0.8$ ). The distance between the two parts is variable and the gaps can be adjusted and tapered independently. At 19.6  $\mu\text{m}$  an optical power of 3 W was outcoupled in a macro pulse of 0.6 ms duration using an electron beam energy of 16.1 MeV and an energy spread of less than 100 keV. The micropulse charge was 50 pC and its width slightly above 1 ps. With the installation of a second acceleration module for additional 20 MeV shorter wavelengths will become available in the near future.

### INTRODUCTION

At Forschungszentrum Rossendorf a superconducting Electron Linac with high Brilliance and low Emittance (ELBE) has been constructed which can deliver a 1 mA cw beam at 40 MeV [1]. The electron beam is used to generate infrared light (Free Electron Lasers), X-rays (electron channelling), MeV-Bremsstrahlung, fast neutrons and positrons. Table 1 gives an overview of the secondary beams at the ELBE facility and the associated fields of science.

### OVERVIEW OF THE ELBE FEL

The ELBE accelerator is fed by a grid-pulsed thermionic gun operating at 250 keV. The gun can deliver 450 ps long pulses and bunch charges up to 77 pC at 13 MHz or 4 pC at 260 MHz. A macro pulser chops the electron beam with adjustable duty cycle and allows to generate a very flexible time structure. By means of two RF buncher cavities operating at 260 MHz and 1.3 GHz the pulses are compressed down to 10 ps upon injection into the first accelerator module.

The Linac uses standing wave RF cavities (1.3 GHz) designed for the TESLA test facility at DESY [2]. Two 9-cell

Table 1: Secondary radiation sources at ELBE and their scientific application

0...20 MeV $\gamma$ -radiation	-nuclear physics -astrophysics
10...100 keV X-rays	-radiation damage of cells -study of phase transitions in liquid metals
5...150 $\mu\text{m}$ infrared FEL	-semiconductor physics -radiochemical and biological experiments
0...30 MeV neutrons	-materials studies for fusion reactors
0...30 keV positrons	-defect studies in solids

superconducting niobium cavities are contained in a cryomodule cooled with superfluid helium at about 2 K. Each cavity has its own RF coupler and is driven by a 10 kW CPI klystron amplifier. The standard accelerating gradient amounts to 10 MeV/m and the beam energy after acceleration is 20 MeV. Downstream the first cryomodule a magnetic chicane is used for bunch length variation. After the installation of the second LINAC module in near future the full energy of ELBE of 40 MeV will be available.

Infrared radiation in the 5–25  $\mu\text{m}$  range will be produced at ELBE in the undulator U27 [3]. It consists of two 34-pole sections with a length of 0.98 m each. The undulator structure has a period of  $\lambda_u=27.3$  mm and consists of NdFeB permanent magnets and poles of decarburized iron (hybride type; the units were test modules for the TTF-Facility at DESY [4] and are modified for use as a “passive” undulator). The sections are mounted on carriages (delivered by DANFYSIK) such that the distance between the two sections is adjustable for phase-matching. The gaps (minimum=13.8 mm, corresponding to  $K_{rms}=0.70$ ) of both sections can be varied independently. For high-gain lasing it is possible to introduce a taper of the field. Both sections were scanned and adjusted using a calibrated Hall probe setup at DESY. After installation at ELBE the field distribution was checked using the pulsed wire method [5]. The inner dimension of 10 x 34 mm<sup>2</sup> of the stainless steel vacuum chamber in the undulator required a well designed resonator. The cavity requirements are summarized in the following Table 2.

To optimize the extraction ratio over the whole wavelength range we use 5 mirrors with different hole sizes in

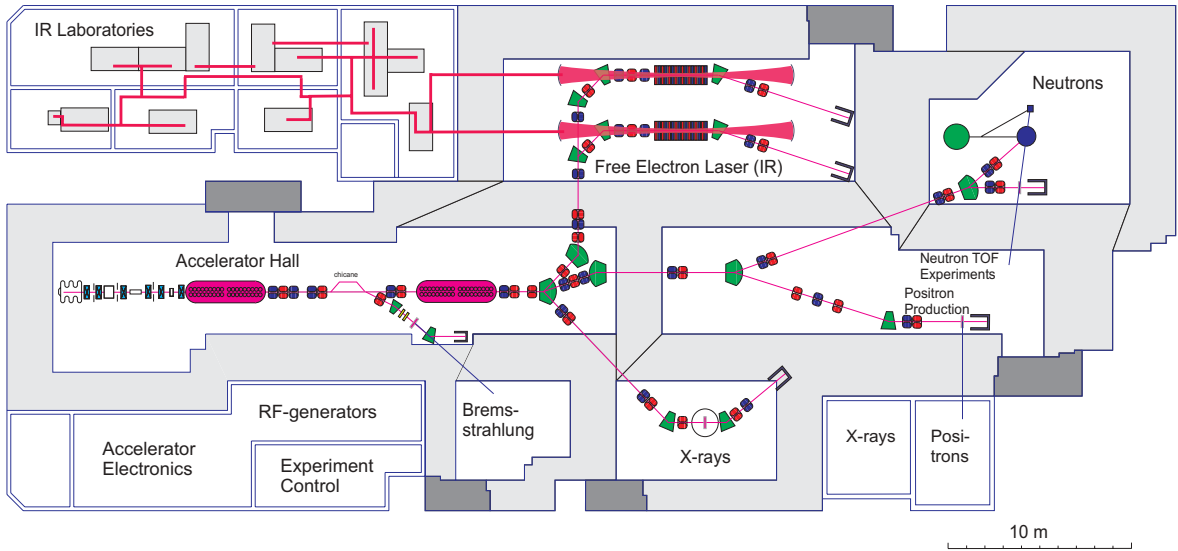


Figure 1: Layout of the radiation source ELBE.

Table 2: Design parameters of the U27 resonator

resonator type	stable, near concentric, symmetric
cavity length	11.53 m, stabilized $< 0.5 \mu\text{m}$
tilt stability	$< 6 \mu\text{rad}$
Rayleigh range	1 m
mirror diameter	7.5 cm
radii of curvature	5.94 m
$g^2$	0.88
diameter of the outcoupling holes	1.5, 2.0, 3.0 and 4.5 mm

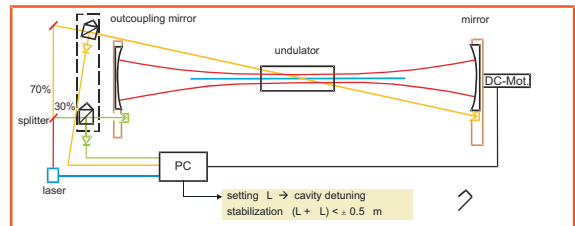


Figure 2: Schematic view of the resonator length control system. Its time constant is one Hz and hence fast in comparison to the thermal time constant of the resonator.

the upstream mirror chamber. The Au-coated Cu-mirrors are mounted on a revolvable holder (wheel), which is fixed to a high-precision rotational stage. Angular adjustment of the mirror wheel is performed using piezoelectric inchworm UHV motors, which provide both coarse and fine adjustments. A similar construction with 3 mirrors of different curvature is used in the downstream chamber. Here, the angular as well as longitudinal adjustment are designed with micrometers and a flexible bar for fine tuning driven by DC-motors outside the vacuum. The translation stage of this mirror will be used to adjust the cavity length to  $< 5 \mu\text{m}$  accuracy.

To ensure the stability of the resonator at wavelengths down to  $3 \mu\text{m}$  we require the mirror angular adjustment to have a resolution and stability in the order of  $6 \mu\text{rad}$ . For the initial alignment of the mirror angles an accuracy in the order of  $20 \mu\text{rad}$  is required. To achieve this accuracy we built an alignment system consisting of two collinear He-Ne lasers using insertable adjustment apertures inside the cavity.

A Hewlett-Packard interferometer system is used to monitor and stabilize the resonator length (see Fig. 2). The interferometer beam is split into two beams (70% and 30%). The low-intensity beam monitors the position of the upstream mirror using one of five retro reflectors installed adjacent to each outcoupling mirror. The high intensity beam passes through the same resonator chamber as the main laser and the electron beam. However, constraints on the width of the vacuum chamber do not leave enough space in the cavity for a separate parallel interferometer beam. Therefore, the latter will pass diagonally from one side of the upstream cavity mirror to a retro reflector on the other side of the downstream mirror. The control electronics for the two interferometer arms include a servo system to control and stabilize the relative distance between the two cavity mirrors using the motorized micrometer drive on the translation stage of the downstream chamber. There is no active tilt stabilization.

Estimating the maximum intracavity laser power, up to 15 W (cw regime) can be absorbed in the mirrors despite

their high reflectivity of more than 99% . To stabilize the mirror wheel temperature we installed a heater in the center of the wheel. Independently of whether the laser is working or not all components are at the same equilibrium temperature slightly above the expected saturation temperature. The mirror wheel is made of Cu to reduce mechanical tension between the mirrors and the surrounding material but thermally isolated from the high-precision rotational stage. The heat is dissipated directly to the outside of the vacuum chamber (Peltier element or air cooling).

Behind the out coupling hole the divergent IR beam passes through a CVD diamond vacuum window (thickness 320  $\mu\text{m}$ ; useable aperture 8 mm) mounted at Brewster angle. The adjacent optical transport system [6] guides the beam to the diagnostic station using 4 (3 toroidal and 1 flat) gold plated copper mirrors. The optics of the system was aligned by monitoring the spatial intensity profiles of a He-Ne guide laser which in turn is aligned to the resonator axis. The same laser will be used for indicating the position of the IR beam in each user laboratory with an accuracy better than 200  $\mu\text{m}$ . Therefore, all optical components of the transport system have to be transparent for IR radiation and for 632 nm as well. Spot size and position of the waist at the diagnostic table are independent of the wavelength. Linear polarization is conserved. The transport system and the diagnostic station [7] both are purged with dry nitrogen to avoid absorption in air. From the main beam, approximately 10...40 percent of the total power are extracted by different beam splitters for wavelength measurement and power monitoring.

## FEL COMMISSIONING

### *Electron beam parameters measurements and diagnostics*

One of the first steps in the FEL commissioning was the electron beam characterization done at a beam energy of 16 MeV. The transverse emittance was measured in the injector with the multislit method, while the emittance of the accelerated beam was measured with the quadrupole scan. At the maximum design bunch charge of 77 pC the emittance is measured to be 8 mm mrad. The gain reduction factor due to the finite emittance was 0.97 at first lasing, i.e., is almost negligible.

Since the FEL gain is linearly proportional to the beam peak current it is highly desirable to minimise the electron bunch length in the vicinity of the undulator. Previously, the bunch length was measured to 1.5 ps (rms) immediately at the accelerator exit using a Martin-Puplett interferometer (MPI). At the undulator with the beam tuned for lasing this value is however different. One can group the beam line elements, which influence the bunch length, between the accelerator exit and the undulator in three groups. These are the magnetic chicane, the “S”-shaped part of the beam line and drift spaces. The chicane can be used to adjust the  $R_{56}$  of the FEL beam line. For the FEL commissioning

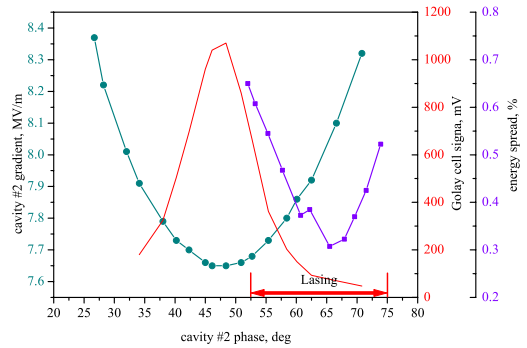


Figure 3: Electron beam parameters dependence on the second cavity phase (dots show the cavity gradient needed for constant energy, squares the energy spread and the line the bunchlength signal).

the MPI was installed right downstream of the undulator. Additionally a single Golay cell detectors was installed upstream of the “S” shaped part of the beam line to measure the total power of the coherent transition radiation, which is in the first approximation inversely proportional to the bunch length. Note that the two Golay cells installed at the interferometer can be used in the same way for the bunch length minimisation without scanning the interferometer. One of the key elements to tune the longitudinal phase space is the second accelerator cavity. Adjusting the cavity phase one changes the electron beam energy spread and the bunch length in the undulator vicinity because of the non-zero  $R_{56}$  of the beam line. For that reason the energy spread and the Golay cell signals were measured as a function of the second cavity phase. Fig. 3 shows results of the measurements. The bunch length at its minimum can be measured with the help of the interferometer. Here the FWHM of the interferogram is about of 2.5 ps.

The most important observation to note is the following: adjusting the cavity phase to have minimum energy spread drastically increases the bunch length in the undulator . In fact at the energy spread minimum the bunch length is so long that it cannot be measured with the MPI. It turns out, however, that for lasing at the used (rather long) wavelength it is more critical to minimize the energy spread of the beam than to minimize the bunchlength.

The electron beam profile and position in the undulator are measured with the help of OTR view screens. They are made of beryllium and have a prism shape. The prism has a 1 mm diameter hole with is precisely aligned to the magnetic axis of the undulator. The view screens are used for the optical cavity alignment as well, which is important to ensure the overlap between the electron beam and the optical mode. It is noteworthy that the view screens are extremely long-term reproducible and reliable, which means that every time an inserted view screen takes the same po-

sition with a  $10\ \mu\text{m}$  accuracy.

ELBE is equipped with a strip-line beam position monitor (BPM) system. The resolution of the system is about  $10\ \mu\text{m}$ . There are two phenomena, which make this system very useful during the FEL operation. First, there is an energy drift observed for the first 2–3 hours every time the linac is switched on. A BPM located in a dispersive region is used to monitor the electron beam energy and to compensate the drift. The second phenomenon is the dependence of the  $R_{56}$  of the “S” shaped beam line on the electron beam path through it. Both phenomena are to be investigated more detailed in the future.

### Observation of the spontaneous radiation

The general idea for the first FEL turn-on was to observe the spontaneous undulator radiation and to maximize it by systematic adjustment of the optical cavity and the electron beam parameters. First, the spontaneous radiation was observed downstream of the undulator so that the optical cavity was not incorporated in the measurements. For that purpose a mirror was inserted in to the beam line behind the last dipole deflecting the beam to the dump. The spontaneous radiation was outcoupled off the beam line through a KRS-5 window and focused by a parabolic mirror on a liquid nitrogen cooled MCT detector. An accurate alignment of the setup was essential for the spontaneous radiation measurements. For the first observation of the spontaneous radiation we had to use an extremely strong averaging of the data, however, that was an important step for the commissioning, since once the spontaneous radiation was observed we could optimize the machine using it as a tune signal.

### Setting the optical cavity length

The adjustment of the FEL cavity to the correct length is an important prerequisite for the achievement of lasing. The cavity length of the FEL has been determined by employing an external frequency stabilized fs mode-locked Ti:sapphire laser (Femtolasers, Austria) [8]. The fs laser is operated at 78.0 MHz, i.e. the 6<sup>th</sup> harmonic of the FEL. A 390 MHz reference signal is derived from the RF electronics of the gun, which is used for stabilizing the repetition rate of the fs laser with a phase-lock loop at its 5<sup>th</sup> harmonic. This synchronization scheme reduces the timing jitter of the fs laser to 500 fs. The pulse train of the fs laser operating at 800 nm with 15 fs pulse duration is directed through the outcoupling hole into the FEL cavity. The light re-emitted through the outcoupling hole is detected via a beam splitter and a fast photodiode. When perfect synchronism of the fs laser and the FEL cavity is achieved, the detected optical pulse is enhanced due to constructive superposition of pulses circulating in the cavity. This results in an increase of the detected pulse intensity by a factor of five. The correct cavity length is determined by this method with an accuracy of some  $\mu\text{m}$ , i.e. a relative accuracy of  $10^{-7}$ . Since the expected FEL operation covers a

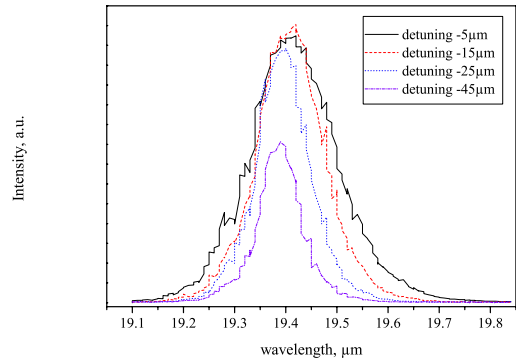


Figure 4: FEL spectra measured at different optical cavity detuning.

cavity detuning range of several  $10\ \mu\text{m}$ , this accuracy was sufficient to start lasing at the preset cavity length.

## FIRST RESULTS

First lasing of the mid-infrared free-electron laser at ELBE was achieved on May 7, 2004. At  $19.6\ \mu\text{m}$  an optical power of 3 W was outcoupled using an macro-pulsed electron beam with an energy of 16.1 MeV and an energy spread of less than 100 keV. The bunch charge was 50 pC.

### The optical spectrum of the FEL

The FEL spectra were measured with a Czerny-Turner type spectrometer (SpectraPro-300i from ARC) which contains a turret with three different gratings (75 l/mm, blazed at  $8\ \mu\text{m}$ ; 60 l/mm, blazed at  $15\ \mu\text{m}$ ; 30 l/mm, blazed at  $30\ \mu\text{m}$ ). For these measurements we used the side exit slit equipped with a single MCT detector. Fig. 4 shows how the spectral width decreases with the detuning of the cavity length.

### Detuning curves

Up to now we operate the FEL in a pulsed mode only using an MCT detector to measure the FEL power as a function of time. In that mode the small signal gain is measured by fitting an exponential function to the rising slope of the MCT signal in its very beginning. The amplitude of the MCT detector close to the macropulse end is associated with the saturated power. The saturation power as well as the small signal gain are measured as a function of the optical cavity detuning. Typical results of such measurements are shown in Fig. 5.

Such measurements are made in the beginning of every FEL run, since the active cavity length stabilization is not yet commissioned and the cavity length may change between the runs. The measured detuning curve appears in

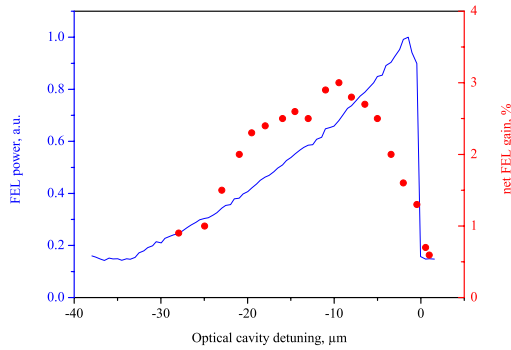


Figure 5: The saturation power (line) and the FEL net gain (dots) vs. optical cavity detuning.

correspondence with the shape predicted by theory. It is also clearly observed that the detuning which optimizes the FEL gain differs from the detuning that optimizes the saturated power, which is also expected according to the theory.

### Optical cavity loss measurements

The optical cavity losses can be measured similar to the small signal gain. At the end of the macropulse the electron beam is turned off instantaneously. Then, the characteristic decay time of the MCT signal carries the information on the cavity losses, which includes diffraction losses at the undulator vacuum chamber as well as the losses on the mirrors and the outcoupled beam. Thus, the total cavity losses were measured as a function of the FEL wavelength. The losses were also calculated using numerical code GLAD. The measurements are in reasonable agreement with the calculations. However, one has to note that the calculations are also limited in accuracy, probably of the same order of magnitude as the measurement accuracy. In the code there is no element like a tube which could simulate the vacuum chamber. For that reason a set of apertures was used to that purpose, which also causes some systematic error. More detailed numerical calculations of the cavity losses are in progress. Results of both the measurements and the calculations are shown in Fig. 6.

### Electron beam energy spectrum

After the electron beam passes the undulator it is deflected to the beam dump by a dipole. There is a quadrupole doublet between the dipole and the dump, which is normally adjusted to have maximum transmission of the electron beam to the dump. However, it can also be also adjusted to image the electron beam energy spectrum on a view screen. Fig. 7 shows both the electron beam energy spectra when the FEL is off and when the FEL turns on. An increase of the energy spread is observed as predicted by Madey's second theorem. The change of the electron

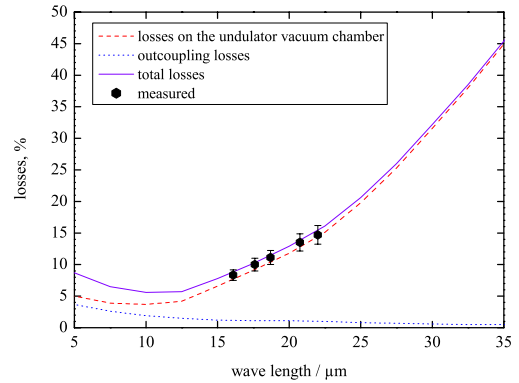


Figure 6: Optical cavity losses.

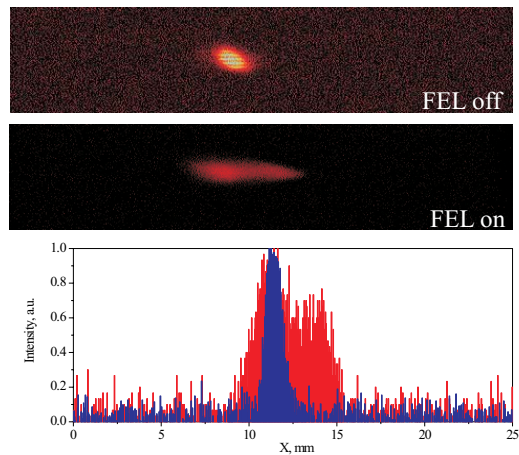


Figure 7: Electron beam spectrum change when the FEL turns on.

beam mean energy is measured as well, which allows one to estimate the amount of energy transferred from the electron beam to the optical beam.

### Autocorrelation IR pulse length measurements

To characterize the ultrashort pulses generated by the FEL we built a non-collinear background-free autocorrelator. As SHG medium we use a CdTe crystal [9]. CdTe is transparent for a wide wavelength range in the FIR, thus, a good candidate for SHG of the FEL radiation.

In Fig. 8 we present the autocorrelation function measured at the maximum-power point of the detuning curve. From the measured autocorrelation we calculate a pulse duration of 2.1 ps, assuming a Gaussian temporal pulse shape. The FWHM of the spectrum is approx. 220 nm. The calculated time-bandwidth product is 0.46 which indicates Fourier-transform limited operation.

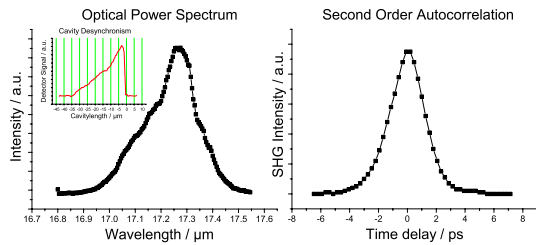


Figure 8: Power spectrum (left) and corresponding SHG autocorrelation (right) at the maximum power point of the cavity detuning curve shown in the insert (left).

## FURTHER DEVELOPMENT

### *The ELBE far-IR FEL*

To produce IR radiation in the THz region (up to 150  $\mu\text{m}$ ) an electromagnetic undulator with an undulator period of 12 cm is envisaged. In this region the FEL constitutes a unique radiation source. Radiation quanta with this energy are appropriate for the spectroscopy of low-energy elementary and collective excitations in solid-state quantum structures and in complex biomolecules as well (e.g. in DNA molecules).

Restricting the electron beam of ELBE to energies above 20 MeV, where the energy spread is better than at lower energies, an undulator with 50 periods guarantees a laser gain of 30%. This undulator should be supplied with a rectangular waveguide which is 10 mm high and extends from the undulator entrance to the downstream resonator mirror. Appropriate mirror curvatures minimize the resonator losses to values below 10%.

### *The ELBE FEL as a user facility*

It is the intention that by the year 2005, the FEL operates as a user facility, being open to users worldwide, provided their scientific proposals have been favorably evaluated by the panel responsible for distribution of beamtime. Under the name "FELBE" the facility is member of the EC funded "Integrating Activity on Synchrotron and Free Electron Laser Science (IA-SFS)", which comprises most synchrotron and FEL facilities in Europe and provides financial support to users from EC and associated states.

The relevant user facilities at FELBE comprise 6 laboratories. Some of these are also used by in-house groups, mainly in the areas of semiconductor physics, biophysics, and radiochemistry, and experiments there will require a certain level of collaboration with the in-house researchers. In particular noteworthy is the fact that a number of other optical sources from the visible to the THz frequency range are available, e.g. for two-color pump-probe experiments. These sources (Ti:sapphire laser and amplifier, OPO, OPA, broad-band THz generator) are all based on Ti:sapphire oscillators which are synchronized with the FEL with an

accuracy better than a ps. Two laboratories are intended to provide users with utmost flexibility for their own experiments, also in scientific areas not covered by in-house groups (e.g., surface physics, molecular physics).

Instructions for beamtime applications will be available on the FELBE website ([www.fz-rossendorf.de/FELBE](http://www.fz-rossendorf.de/FELBE)) by the end of 2004.

## ACKNOWLEDGEMENTS

The authors would like to thank the colleagues from HEPL Stanford University, DESY Hamburg, Jlab Newport News and FELIX Nieuwegein for strong help and useful discussions. Special thanks to Prof. Todd Smith, A.F.G. van der Meer and Kevin Jordan.

## REFERENCES

- [1] F. Gabriel et al., NIM B 161–163 (2000), 1143–1147
- [2] TESLA Test Facility Linac – Design Report (Ed. D.A. Edwards), DESY print TESLA 95–01
- [3] P. Gippner et al., Contribution to the 23rd Int. Free Electron Laser Conf. Darmstadt, Germany, 2001, Nucl. Instr. and Meth. A483 (2002) II–55
- [4] B. Faatz, J. Pflüger and Y.M. Nikitina, Nucl. Instr. Meth. A 375 (1996) 618
- [5] P. Evtushenko et al., Contribution to the 25th Int. Free Electron Laser Conf. Tzukuba, Japan, 2003
- [6] Th. Dekorsy et al., Contribution to the 24th Int. Free Electron Laser Conf. Argonne, USA, 2002, Nucl. Instr. and Meth. A507 (2003) II–35
- [7] W. Seidel et al., Annual Report 2001, FZR–341 (2002) 34
- [8] K.W. Berryman, P. Haar, and B.A. Richman, Nucl. Instr. Meth. A 358 (1995) 260–263
- [9] J. Xu, G.M.H. Knippels, D. Oepts, and A.F.G. van der Meer, Opt. Comm. 197 (2001) 379–383